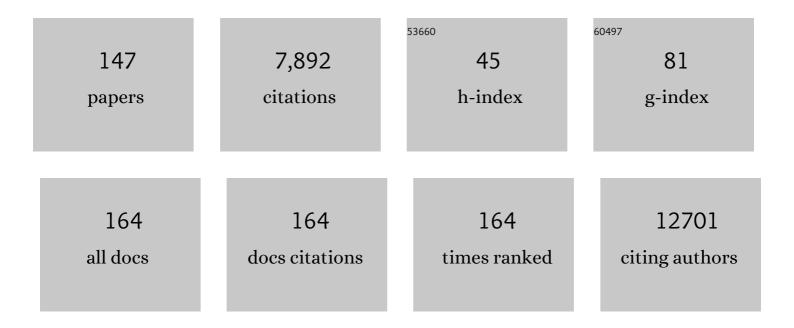
Tobias Madl

List of Publications by Year in descending order

Source: https://exaly.com/author-pdf/7049224/publications.pdf Version: 2024-02-01



TORIAS MADI

#	Article	IF	CITATIONS
1	Fasting improves therapeutic response in hepatocellular carcinoma through p53-dependent metabolic synergism. Science Advances, 2022, 8, eabh2635.	4.7	35
2	Oral Intake of L-Ornithine-L-Aspartate Is Associated with Distinct Microbiome and Metabolome Changes in Cirrhosis. Nutrients, 2022, 14, 748.	1.7	2
3	EGCG Promotes FUS Condensate Formation in a Methylation-Dependent Manner. Cells, 2022, 11, 592.	1.8	3
4	Cohort profile: â€~Biomarkers of Personalised Medicine' (BioPersMed): a single-centre prospective observational cohort study in Graz/Austria to evaluate novel biomarkers in cardiovascular and metabolic diseases. BMJ Open, 2022, 12, e058890.	0.8	6
5	Patterns of Peripheral Blood B-Cell Subtypes Are Associated With Treatment Response in Patients Treated With Immune Checkpoint Inhibitors: A Prospective Longitudinal Pan-Cancer Study. Frontiers in Immunology, 2022, 13, 840207.	2.2	7
6	Metabolomic Profiles of Mouse Tissues Reveal an Interplay between Aging and Energy Metabolism. Metabolites, 2022, 12, 17.	1.3	10
7	A General Small-Angle X-ray Scattering-Based Screening Protocol for Studying Physical Stability of Protein Formulations. Pharmaceutics, 2022, 14, 69.	2.0	3
8	FOXO transcription factors differ in their dynamics and intra/intermolecular interactions. Current Research in Structural Biology, 2022, 4, 118-133.	1.1	7
9	Complementary omics strategies to dissect p53 signaling networks under nutrient stress. Cellular and Molecular Life Sciences, 2022, 79, .	2.4	4
10	HDL-apoA-II Is Strongly Associated with 1-Year Mortality in Acute Heart Failure Patients. Biomedicines, 2022, 10, 1668.	1.4	6
11	βâ€catenin regulates FOXP2 transcriptional activity via multiple binding sites. FEBS Journal, 2021, 288, 3261-3284.	2.2	11
12	Endothelial Lipase Modulates Paraoxonase 1 Content and Arylesterase Activity of HDL. International Journal of Molecular Sciences, 2021, 22, 719.	1.8	9
13	Tissue-Specific Landscape of Metabolic Dysregulation during Ageing. Biomolecules, 2021, 11, 235.	1.8	24
14	Lysophosphatidic Acid Induces Aerobic Glycolysis, Lipogenesis, and Increased Amino Acid Uptake in BV-2 Microglia. International Journal of Molecular Sciences, 2021, 22, 1968.	1.8	10
15	NLRP3 as a sensor of metabolism gone awry. Current Opinion in Biotechnology, 2021, 68, 300-309.	3.3	8
16	Dietary spermidine improves cognitive function. Cell Reports, 2021, 35, 108985.	2.9	98
17	Metabolic, Phenotypic, and Neuropathological Characterization of the Tg4-42 Mouse Model for Alzheimer's Disease. Journal of Alzheimer's Disease, 2021, 80, 1151-1168.	1.2	5
18	Potassium ions promote hexokinase-II dependent glycolysis. IScience, 2021, 24, 102346.	1.9	12

#	Article	IF	CITATIONS
19	Growing Human Hepatocellular Tumors Undergo a Global Metabolic Reprogramming. Cancers, 2021, 13, 1980.	1.7	9
20	ATP regulates RNAâ€driven cold inducible RNA binding protein phase separation. Protein Science, 2021, 30, 1438-1453.	3.1	18
21	Global analysis of protein arginine methylation. Cell Reports Methods, 2021, 1, 100016.	1.4	27
22	Wide-Range, Rapid, and Specific Identification of Pathogenic Bacteria by Surface-Enhanced Raman Spectroscopy. ACS Sensors, 2021, 6, 2911-2919.	4.0	39
23	Multiple regulatory intrinsically disordered motifs control FOXO4 transcription factor binding and function. Cell Reports, 2021, 36, 109446.	2.9	27
24	Metabolic profiling links cardiovascular risk and vascular end organ damage. Atherosclerosis, 2021, 331, 45-53.	0.4	7
25	Branched-Chain Amino Acids Can Predict Mortality in ICU Sepsis Patients. Nutrients, 2021, 13, 3106.	1.7	19
26	Structural and DNA-binding properties of the cytoplasmic domain of Vibrio cholerae transcription factor ToxR. Journal of Biological Chemistry, 2021, 297, 101167.	1.6	5
27	Reduced B12 uptake and increased gastrointestinal formate are associated with archaeome-mediated breath methane emission in humans. Microbiome, 2021, 9, 193.	4.9	24
28	Intracellular drug binding affinities by NMR. Acta Crystallographica Section D: Structural Biology, 2021, 77, 1216-1217.	1.1	0
29	Imbalances in the eye lens proteome are linked to cataract formation. Nature Structural and Molecular Biology, 2021, 28, 143-151.	3.6	26
30	p53 Transactivation Domain Mediates Binding and Phase Separation with Poly-PR/GR. International Journal of Molecular Sciences, 2021, 22, 11431.	1.8	9
31	Phosphorylation Regulates CIRBP Arginine Methylation, Transportin-1 Binding and Liquid-Liquid Phase Separation. Frontiers in Molecular Biosciences, 2021, 8, 689687.	1.6	12
32	XIAP restrains TNF-driven intestinal inflammation and dysbiosis by promoting innate immune responses of Paneth and dendritic cells. Science Immunology, 2021, 6, eabf7235.	5.6	17
33	Activation of efficient DNA repair mechanisms after photon and proton irradiation of human chondrosarcoma cells. Scientific Reports, 2021, 11, 24116.	1.6	5
34	Exploring the Arginine Methylome by Nuclear Magnetic Resonance Spectroscopy. Journal of Visualized Experiments, 2021, , .	0.2	4
35	Low cardiac lipolysis reduces mitochondrial fission and prevents lipotoxic heart dysfunction in Perilipin 5 mutant mice. Cardiovascular Research, 2020, 116, 339-352.	1.8	23
36	A small molecule chaperone rescues the stability and activity of a cancerâ€associated variant of NAD(P)H:quinone oxidoreductase 1 <i>inÂvitro</i> . FEBS Letters, 2020, 594, 424-438.	1.3	7

#	Article	IF	CITATIONS
37	Cysteine oxidation triggers amyloid fibril formation of the tumor suppressor p16INK4A. Redox Biology, 2020, 28, 101316.	3.9	17
38	Transgene integration causes RARB downregulation in homozygous Tg4–42 mice. Scientific Reports, 2020, 10, 6377.	1.6	5
39	Tin-Doped Near-Infrared Persistent Luminescence Nanoparticles with Considerable Improvement of Biological Window Activation for Deep Tumor Photodynamic Therapy. ACS Applied Bio Materials, 2020, 3, 5995-6004.	2.3	15
40	Metabolic reprogramming of donor T cells enhances graft-versus-leukemia effects in mice and humans. Science Translational Medicine, 2020, 12, .	5.8	70
41	Nuclear Import Receptors Directly Bind to Arginine-Rich Dipeptide Repeat Proteins and Suppress Their Pathological Interactions. Cell Reports, 2020, 33, 108538.	2.9	69
42	Human Milk Oligosaccharides Modulate the Risk for Preterm Birth in a Microbiome-Dependent and -Independent Manner. MSystems, 2020, 5, .	1.7	10
43	Dipeptidyl peptidase 3 modulates the renin–angiotensin system in mice. Journal of Biological Chemistry, 2020, 295, 13711-13723.	1.6	34
44	Probing Surfaces in Dynamic Protein Interactions. Journal of Molecular Biology, 2020, 432, 2949-2972.	2.0	17
45	Structure of an RNA aptamer in complex with the fluorophore tetramethylrhodamine. Nucleic Acids Research, 2020, 48, 949-961.	6.5	12
46	Nonclassical nuclear localization signals mediate nuclear import of CIRBP. Proceedings of the National Academy of Sciences of the United States of America, 2020, 117, 8503-8514.	3.3	40
47	Purification and Application of Genetically Encoded Potassium Ion Indicators for Quantification of Potassium Ion Concentrations within Biological Samples. Current Protocols in Chemical Biology, 2019, 11, e71.	1.7	3
48	NMR characterization of solvent accessibility and transient structure in intrinsically disordered proteins. Journal of Biomolecular NMR, 2019, 73, 305-317.	1.6	30
49	Glycogen Synthase Kinase 3 Beta Controls Presenilin-1-Mediated Endoplasmic Reticulum Ca2+ Leak Directed to Mitochondria in Pancreatic Islets and beta-Cells. Cellular Physiology and Biochemistry, 2019, 52, 57-75.	1.1	25
50	Alternate Day Fasting Improves Physiological and Molecular Markers of Aging in Healthy, Non-obese Humans. Cell Metabolism, 2019, 30, 462-476.e6.	7.2	256
51	Acetyl-CoA carboxylase 1–dependent lipogenesis promotes autophagy downstream of AMPK. Journal of Biological Chemistry, 2019, 294, 12020-12039.	1.6	29
52	Endothelial lipase increases antioxidative capacity of high-density lipoprotein. Biochimica Et Biophysica Acta - Molecular and Cell Biology of Lipids, 2019, 1864, 1363-1374.	1.2	19
53	Serum Concentrations of Citrate, Tyrosine, 2- and 3- Hydroxybutyrate are Associated with Increased 3-Month Mortality in Acute Heart Failure Patients. Scientific Reports, 2019, 9, 6743.	1.6	23
54	Increased Aggregation Tendency of Alpha-Synuclein in a Fully Disordered Protein Complex. Journal of Molecular Biology, 2019, 431, 2581-2598.	2.0	22

#	Article	IF	CITATIONS
55	The Co-chaperone Cns1 and the Recruiter Protein Hgh1 Link Hsp90 to Translation Elongation via Chaperoning Elongation Factor 2. Molecular Cell, 2019, 74, 73-87.e8.	4.5	22
56	pH-Lemon, a Fluorescent Protein-Based pH Reporter for Acidic Compartments. ACS Sensors, 2019, 4, 883-891.	4.0	99
57	Impaired Retinal Vessel Dilation Predicts Mortality in End-Stage Renal Disease. Circulation Research, 2019, 124, 1796-1807.	2.0	44
58	A single alcohol binge impacts on neutrophil function without changes in gut barrier function and gut microbiome composition in healthy volunteers. PLoS ONE, 2019, 14, e0211703.	1.1	23
59	Enhanced inter-compartmental Ca2+ flux modulates mitochondrial metabolism and apoptotic threshold during aging. Redox Biology, 2019, 20, 458-466.	3.9	50
60	N-acetylaspartate pathway is nutrient responsive and coordinates lipid and energy metabolism in brown adipocytes. Biochimica Et Biophysica Acta - Molecular Cell Research, 2019, 1866, 337-348.	1.9	37
61	Presenilin-1 Established ER-Ca2+ Leak: a Follow Up on Its Importance for the Initial Insulin Secretion in Pancreatic Islets and β-Cells Upon Elevated Glucose. Cellular Physiology and Biochemistry, 2019, 53, 573-586.	1.1	15
62	Regulation of cellular senescence <i>via</i> the <scp>FOXO</scp> 4â€p53 axis. FEBS Letters, 2018, 592, 2083-2097.	1.3	73
63	A switch point in the molecular chaperone Hsp90 responding to client interaction. Nature Communications, 2018, 9, 1472.	5.8	30
64	Phase Separation of FUS Is Suppressed by Its Nuclear Import Receptor and Arginine Methylation. Cell, 2018, 173, 706-719.e13.	13.5	484
65	Lysyl oxidase-like protein 2 (LOXL2) modulates barrier function in cholangiocytes in cholestasis. Journal of Hepatology, 2018, 69, 368-377.	1.8	27
66	P2â€238: INTEGRATIVE CHARACTERIZATION OF A RODENT ALZHEIMER'S DISEASE MODEL. Alzheimer's and Dementia, 2018, 14, P762.	0.4	0
67	Saxagliptin but Not Sitagliptin Inhibits CaMKII and PKC via DPP9 Inhibition in Cardiomyocytes. Frontiers in Physiology, 2018, 9, 1622.	1.3	17
68	Oxidative stress induced structural changes in the microtubuleâ€associated flavoenzyme Irc15p from Saccharomyces cerevisiae. Protein Science, 2018, 28, 176-190.	3.1	1
69	NMR spectroscopy enables simultaneous quantification of carbohydrates for diagnosis of intestinal and gastric permeability. Scientific Reports, 2018, 8, 14650.	1.6	13
70	The neuronal S100B protein is a calcium-tuned suppressor of amyloid-β aggregation. Science Advances, 2018, 4, eaaq1702.	4.7	49
71	Entspannte Moleküle: NMR-Ober - flÜhen daten zur Strukturbestimmung. BioSpektrum, 2018, 24, 161-163.	0.0	0
72	Cytosolic Aspartate Availability Determines Cell Survival When Glutamine Is Limiting. Cell Metabolism, 2018, 28, 706-720.e6.	7.2	132

#	Article	IF	CITATIONS
73	Acetate-free, citrate-acidified bicarbonate dialysis improves serum calcification propensity—a preliminary study. Nephrology Dialysis Transplantation, 2018, 33, 2043-2051.	0.4	28
74	Small Paramagnetic Co-solute Molecules. New Developments in NMR, 2018, , 283-309.	0.1	7
75	Metabolic Reprogramming Overcomes T Cell Inhibition By AML Cells. Blood, 2018, 132, 3328-3328.	0.6	0
76	Catalytic competence, structure and stability of the cancerâ€associated R139W variant of the human <scp>NAD</scp> (P)H:quinone oxidoreductase 1 (<scp>NQO</scp> 1). FEBS Journal, 2017, 284, 1233-1245.	2.2	30
77	Long-range allosteric signaling in red light–regulated diguanylyl cyclases. Science Advances, 2017, 3, e1602498.	4.7	87
78	Flexible IgE epitope-containing domains of Phl p 5 cause high allergenic activity. Journal of Allergy and Clinical Immunology, 2017, 140, 1187-1191.	1.5	19
79	Targeted Apoptosis of Senescent Cells Restores Tissue Homeostasis in Response to Chemotoxicity and Aging. Cell, 2017, 169, 132-147.e16.	13.5	979
80	Allosteric modulation of peroxisomal membrane protein recognition by farnesylation of the peroxisomal import receptor PEX19. Nature Communications, 2017, 8, 14635.	5.8	47
81	The redox environment triggers conformational changes and aggregation of hIAPP in Type II Diabetes. Scientific Reports, 2017, 7, 44041.	1.6	75
82	EL-HDL exhibits increased capacity to attenuate LDL oxidation independent of pon1. Atherosclerosis, 2017, 263, e216.	0.4	0
83	RNA structure refinement using NMR solvent accessibility data. Scientific Reports, 2017, 7, 5393.	1.6	26
84	Patchy proteins form a perfect lens. Science, 2017, 357, 546-547.	6.0	6
85	Characterization of Protein–Protein Interfaces in Large Complexes by Solid-State NMR Solvent Paramagnetic Relaxation Enhancements. Journal of the American Chemical Society, 2017, 139, 12165-12174.	6.6	35
86	Novel genetically encoded fluorescent probes enable real-time detection of potassium in vitro and in vivo. Nature Communications, 2017, 8, 1422.	5.8	130
87	Liver p53 is stabilized upon starvation and required for amino acid catabolism and gluconeogenesis. FASEB Journal, 2017, 31, 732-742.	0.2	55
88	[P2–229]: NMRâ€BASED METABOLIC PHENOTYPING OF RODENT ALZHEIMER's DISEASE MODELS. Alzheimer's and Dementia, 2017, 13, P698.	0.4	0
89	Transient helicity in intrinsically disordered Axin-1 studied by NMR spectroscopy and molecular dynamics simulations. PLoS ONE, 2017, 12, e0174337.	1.1	7
90	Integrative metabolomics as emerging tool to study autophagy regulation. Microbial Cell, 2017, 4, 240-258.	1.4	18

#	Article	IF	CITATIONS
91	Randomised clinical trial: the effects of a multispecies probiotic vs. placebo on innate immune function, bacterial translocation and gut permeability in patients with cirrhosis. Alimentary Pharmacology and Therapeutics, 2016, 44, 926-935.	1.9	89
92	Crystal and solution structural studies of mouse phospholipid hydroperoxide glutathione peroxidase 4. Acta Crystallographica Section F, Structural Biology Communications, 2016, 72, 743-749.	0.4	19
93	Importance of cycle timing for the function of the molecular chaperone Hsp90. Nature Structural and Molecular Biology, 2016, 23, 1020-1028.	3.6	78
94	Prediction of Protein Structure Using Surface Accessibility Data. Angewandte Chemie - International Edition, 2016, 55, 11970-11974.	7.2	31
95	PRMT1-mediated methylation of MICU1 determines the UCP2/3 dependency of mitochondrial Ca2+ uptake in immortalized cells. Nature Communications, 2016, 7, 12897.	5.8	59
96	Increasing the Chemicalâ€Shift Dispersion of Unstructured Proteins with a Covalent Lanthanide Shift Reagent. Angewandte Chemie - International Edition, 2016, 55, 14847-14851.	7.2	29
97	Recognition of the 3′ splice site RNA by the U2AF heterodimer involves a dynamic population shift. Proceedings of the National Academy of Sciences of the United States of America, 2016, 113, E7169-E7175.	3.3	57
98	Prediction of Protein Structure Using Surface Accessibility Data. Angewandte Chemie, 2016, 128, 12149-12153.	1.6	1
99	Verbesserung der Dispersion der chemischen Verschiebungen von unstrukturierten Proteinen durch einen kovalent gebundenen Lanthanoidkomplex. Angewandte Chemie, 2016, 128, 15069-15073.	1.6	1
100	Lysosomal acid lipase regulates VLDL synthesis and insulin sensitivity in mice. Diabetologia, 2016, 59, 1743-1752.	2.9	37
101	Monomethylated and unmethylated FUS exhibit increased binding to Transportin and distinguish FTLD-FUS from ALS-FUS. Acta Neuropathologica, 2016, 131, 587-604.	3.9	76
102	Axin cancer mutants form nanoaggregates to rewire the Wnt signaling network. Nature Structural and Molecular Biology, 2016, 23, 324-332.	3.6	31
103	Structural basis of nucleic-acid recognition and double-strand unwinding by the essential neuronal protein Pur-alpha. ELife, 2016, 5, .	2.8	35
104	Optimization of lipid production with a genome-scale model of Yarrowia lipolytica. BMC Systems Biology, 2015, 9, 72.	3.0	101
105	The activity of protein phosphatase 5 towards native clients is modulated by the middle- and C-terminal domains of Hsp90. Scientific Reports, 2015, 5, 17058.	1.6	29
106	Hop/Sti1 phosphorylation inhibits its coâ€chaperone function. EMBO Reports, 2015, 16, 240-249.	2.0	30
107	Typeâ€ <scp>II NADH</scp> :quinone oxidoreductase from S <i>taphylococcus aureus</i> has two distinct binding sites and is rate limited by quinone reduction. Molecular Microbiology, 2015, 98, 272-288.	1.2	39
108	A Crystallin Fold in the Interleukin-4-inducing Principle of Schistosoma mansoni Eggs (IPSE/α-1) Mediates IgE Binding for Antigen-independent Basophil Activation. Journal of Biological Chemistry, 2015, 290, 22111-22126.	1.6	29

#	Article	IF	CITATIONS
109	A Compact Native 24-Residue Supersecondary Structure Derived from the Villin Headpiece Subdomain. Biophysical Journal, 2015, 108, 678-686.	0.2	7
110	Introduction of germline residues improves the stability of anti-HIV mAb 2G12-IgM. Biochimica Et Biophysica Acta - Proteins and Proteomics, 2015, 1854, 1536-1544.	1.1	7
111	AAA+ chaperones and acyldepsipeptides activate the ClpP protease via conformational control. Nature Communications, 2015, 6, 6320.	5.8	110
112	The Solution Structure of the Lantibiotic Immunity Protein Nisl and Its Interactions with Nisin. Journal of Biological Chemistry, 2015, 290, 28869-28886.	1.6	34
113	Hsp90 regulates the dynamics of its cochaperone Sti1 and the transfer of Hsp70 between modules. Nature Communications, 2015, 6, 6655.	5.8	76
114	Solution PRE NMR. Biological Magnetic Resonance, 2015, , 133-157.	0.4	3
115	Modulation of the Hsp90 Chaperone Cycle by a Stringent Client Protein. Molecular Cell, 2014, 53, 941-953.	4.5	129
116	A Novel Pex14 Protein-interacting Site of Human Pex5 Is Critical for Matrix Protein Import into Peroxisomes. Journal of Biological Chemistry, 2014, 289, 437-448.	1.6	60
117	Hsp90-Tau Complex Reveals Molecular Basis for Specificity in Chaperone Action. Cell, 2014, 156, 963-974.	13.5	269
118	Transient Electrostatic Interactions Dominate the Conformational Equilibrium Sampled by Multidomain Splicing Factor U2AF65: A Combined NMR and SAXS Study. Journal of the American Chemical Society, 2014, 136, 7068-7076.	6.6	79
119	NMR approaches for structural analysis of multidomain proteins and complexes in solution. Progress in Nuclear Magnetic Resonance Spectroscopy, 2014, 80, 26-63.	3.9	164
120	Redox-Dependent Control of FOXO/DAF-16 by Transportin-1. Molecular Cell, 2013, 49, 730-742.	4.5	138
121	High-resolution structures of the IgM Fc domains reveal principles of its hexamer formation. Proceedings of the National Academy of Sciences of the United States of America, 2013, 110, 10183-10188.	3.3	73
122	Structure, phosphorylation and U2AF65 binding of the N-terminal domain of splicing factor 1 during 3′-splice site recognition. Nucleic Acids Research, 2013, 41, 1343-1354.	6.5	61
123	Studying the Structure and Dynamics of Biomolecules by Using Soluble Paramagnetic Probes. ChemPhysChem, 2013, 14, 3082-3094.	1.0	54
124	Arginine methylation next to the PY-NLS modulates Transportin binding and nuclear import of FUS. EMBO Journal, 2012, 31, 4258-4275.	3.5	266
125	hnRNP A1 Proofreads 3′ Splice Site Recognition by U2AF. Molecular Cell, 2012, 45, 314-329.	4.5	87
126	In support of the BMRB. Nature Structural and Molecular Biology, 2012, 19, 854-860.	3.6	6

#	Article	IF	CITATIONS
127	Multi-domain conformational selection underlies pre-mRNA splicing regulation by U2AF. Nature, 2011, 475, 408-411.	13.7	202
128	Structural basis for dimethylarginine recognition by the Tudor domains of human SMN and SPF30 proteins. Nature Structural and Molecular Biology, 2011, 18, 1414-1420.	3.6	164
129	NMR and small-angle scattering-based structural analysis of protein complexes in solution. Journal of Structural Biology, 2011, 173, 472-482.	1.3	67
130	Structural Analysis of Large Protein Complexes Using Solvent Paramagnetic Relaxation Enhancements. Angewandte Chemie - International Edition, 2011, 50, 3993-3997.	7.2	71
131	A Radical Approach to Hydroxylaminotrichlorosilanes: Synthesis, Reactivity, and Crystal Structure of TEMPO‧iCl ₃ (TEMPO = 2,2,6,6â€Tetramethylpiperidineâ€ <i>N</i> â€oxyl). European Journal of Inorganic Chemistry, 2010, 2010, 289-297.	1.0	26
132	An Efficient Protocol for NMR‧pectroscopyâ€Based Structure Determination of Protein Complexes in Solution. Angewandte Chemie - International Edition, 2010, 49, 1967-1970.	7.2	104
133	NES consensus redefined by structures of PKI-type and Rev-type nuclear export signals bound to CRM1. Nature Structural and Molecular Biology, 2010, 17, 1367-1376.	3.6	226
134	Structural Basis for Homodimerization of the Src-associated during Mitosis, 68-kDa Protein (Sam68) Qua1 Domain. Journal of Biological Chemistry, 2010, 285, 28893-28901.	1.6	37
135	Structural Analysis of Protein Interfaces from 13C Direct-Detected Paramagnetic Relaxation Enhancements. Journal of the American Chemical Society, 2010, 132, 7285-7287.	6.6	31
136	Adhesion Dance with Raver. Structure, 2009, 17, 781-783.	1.6	7
137	Use of Relaxation Enhancements in a Paramagnetic Environment for the Structure Determination of Proteins Using NMR Spectroscopy. Angewandte Chemie - International Edition, 2009, 48, 8259-8262.	7.2	84
138	Structural basis for competitive interactions of Pex14 with the import receptors Pex5 and Pex19. EMBO Journal, 2009, 28, 745-754.	3.5	82
139	Positioning of Micelle-Bound Peptides by Paramagnetic Relaxation Enhancements. Journal of Physical Chemistry B, 2009, 113, 4400-4406.	1.2	47
140	Synthesis of Naturally Occurring Arsenic-Containing Carbohydrates. Australian Journal of Chemistry, 2009, 62, 538.	0.5	15
141	Relax with TEMPO: A Paramagnetic Relaxation Agent Useful also for Silicon-29 NMR Spectroscopy. Organometallics, 2008, 27, 500-502.	1.1	11
142	Mapping the Orientation of Helices in Micelle-Bound Peptides by Paramagnetic Relaxation Waves. Journal of the American Chemical Society, 2007, 129, 5228-5234.	6.6	119
143	Structural Basis for Nucleic Acid and Toxin Recognition of the Bacterial Antitoxin CcdA. Journal of Molecular Biology, 2006, 364, 170-185.	2.0	119
144	Tandem mass spectrometric analysis of a complex triterpene saponin mixture of Chenopodium quinoa. Journal of the American Society for Mass Spectrometry, 2006, 17, 795-806.	1.2	130

#	Article	IF	CITATIONS
145	Quantification of primary fatty acid amides in commercial tallow and tallow fatty acid methyl esters by HPLC-APCI-MS. Analyst, The, 2005, 130, 565.	1.7	14
146	Hexokinase-II Enzymatic Activity Requires High Levels of Intracellular K+. SSRN Electronic Journal, 0, , .	0.4	0
147	p53 Regulates a miRNA-Fructose Transporter Axis in Brown Adipose Tissue Under Fasting. Frontiers in Genetics, 0, 13, .	1.1	2